Dehydrogenative Synthesis of Carboxylic Acids from Primary Alcohols and Hydroxide Catalyzed by a Ruthenium N-Heterocyclic Carbene Complex

Santilli, Carola; Makarov, Ilya; Fristrup, Peter; Madsen, Robert

Published in:
The Journal of Organic Chemistry

Link to article, DOI:
10.1021/acs.joc.6b02105

Publication date:
2016

Document Version
Peer reviewed version

Dehydrogenative Synthesis of Carboxylic Acids from Primary Alcohols and Hydroxide Catalyzed by a Ruthenium N-Heterocyclic Carbene Complex

Carola Santilli, Ilya S. Makarov, Peter Fristrup and Robert Madsen*

Department of Chemistry, Technical University of Denmark, DK-2800 Lyngby, Denmark

E-mail: rm@kemi.dtu.dk

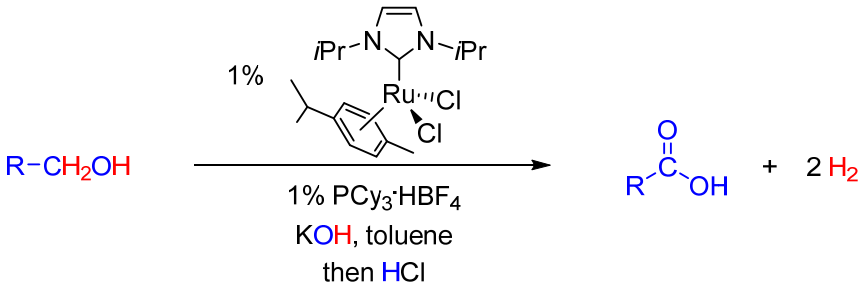

Abstract

Primary alcohols have been reacted with hydroxide and the ruthenium complex [$RuCl_2$(I*i*Pr)(*p*-cymene)] to afford carboxylic acids and dihydrogen. The dehydrogenative reaction is performed in toluene which allows for a simple isolation of the products by precipitation and extraction. The transformation can be applied to a range of benzylic and saturated aliphatic alcohols containing halide and (thio)ether substituents while olefins and ester groups are not compatible with the reaction conditions. Benzylic alcohols undergo faster conversion than other substrates and a competing Cannizzaro reaction is most likely involved in this case. The kinetic isotope effect was determined to be 0.67 by using 1-butanol as the substrate. A plausible catalytic cycle was characterized by DFT/B3LYP-D3 and involved coordination of the alcohol to the metal, β-

hydride elimination, hydroxide attack on the coordinated aldehyde and a second β-hydride elimination to furnish the carboxylate.

INTRODUCTION

The oxidation of a primary alcohol to a carboxylic acid constitutes one of the fundamental textbook reactions in organic chemistry. The oxidation is usually carried out with a stoichiometric metal oxide or by a catalytic procedure where either a metal, a metal complex or an organic molecule serves as the catalyst in the presence of a cheap stoichiometric oxidant such as dioxygen, periodate or hypochlorite.[1]

In recent years, dehydrogenation with the liberation of dihydrogen has gained significant attention as an alternative method for the oxidation of alcohols. This has led to very efficient syntheses of amides, imines, esters and acetals from primary alcohols where no stoichiometric additive or oxidant is employed and with dihydrogen as the only byproduct.[2] The transformations are usually carried out in the presence of various ruthenium complexes which dehydrogenate the primary alcohol to the corresponding aldehyde. Subsequent reaction with an amine or an alcohol furnishes imines and acetals while amides and esters are obtained when the transformation is accompanied by another dehydrogenation.[2]

If water is employed as the nucleophile the dehydrogenation from a primary alcohol may form the corresponding carboxylic acid. The development of this transformation, however, has been more slow. First, several rhodium complexes with a diolefin amido ligand were shown to catalyze the oxidation, but the reaction required a ketone, an alkene, dioxygen or nitrous oxide as a hydrogen scavenger.[3] In 2013, 0.2% of a ruthenium PNN pincer complex was employed to

catalyze the oxidation in aqueous solution in the absence of a hydrogen scavenger[4] and the reaction has recently been extended to the synthesis of amino acids from amino alcohols.[5] The mechanism of this transformation has been studied computationally and the reaction was shown to proceed through the aldehyde which reacts with water to form a gem-diol followed by dehydrogenation to the carboxylic acid.[6] Since then, 1% of a ruthenium benzimidazolylidene complex[7] and 0.1 – 1% of several ruthenium PNP pincer complexes[8] were presented as catalysts for the oxidation under analogous conditions and it was shown that ruthenium carbonyl complexes may be formed during the reaction by decarbonylation of the aldehyde.[8b] In the same way, aqueous ethanol has been subjected to the catalytic dehydrogenation with similar ruthenium PNP pincer complexes in order to produce dihydrogen from a renewable alcohol.[9] Palladium on carbon has also been applied as a catalyst with a 5 mol% palladium loading for the carboxylic acid synthesis where a reduced pressure was necessary in order to achieve a good yield.[10] In all these oxidations of primary alcohols to carboxylic acids a stoichiometric amount of sodium hydroxide is included and the immediate product is therefore the sodium salt of the acid. This makes the overall transformation energetically more favored and prevents deactivation of the catalyst by the acid as well as formation of the ester by a competing pathway.[6] Furthermore, the dehydrogenations are all performed with water as the solvent which in some cases constitute a limitation in the oxidation of more lipophilic alcohols.[7,8]

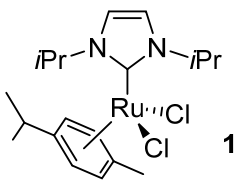

1

Figure 1. Structure of complex **1**.

In 2008 we introduced ruthenium N-heterocyclic carbene complexes for the dehydrogenation of primary alcohols and complex **1** has been used as a (pre)catalyst for the synthesis of amides,[11] esters[12] and imines (Figure 1).[13] The mechanism for the formation of amides has been studied in detail by experimental and theoretical methods where it has been shown that both the aldehyde and the hemiaminal intermediate stay coordinated to the metal during the catalytic cycle.[14] We envisioned that this transformation could be extended to the formation of carboxylic acids by performing the dehydrogenation in the presence of water or hydroxide. Herein, we report a full account on the dehydrogenative synthesis of carboxylic acids with complex **1** and describe a theoretical investigation of the reaction mechanism.

RESULTS AND DISCUSSION

The formation of a carboxylic acid was first observed during our optimization of the ester synthesis from primary alcohols. The optimized conditions for this transformation required 1 – 5% of **1**, 1 – 5% of PCy_3, 3 – 15% of KO*t*Bu and a strong base (Mg_3N_2 or K_3PO_4) in refluxing toluene,[12a] but when the bases were replaced by a stoichiometric amount of KOH the corresponding carboxylic acid was obtained. In this way, 2-phenylethanol was converted into phenylacetic acid in 75% yield (Scheme 1).

Scheme 1. Conditions for Dehydrogenative Oxidation of Primary Alcohols

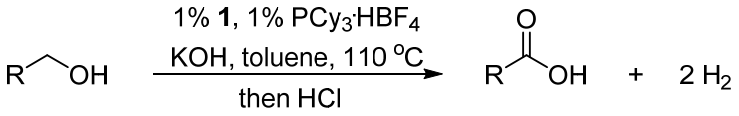

R = $PhCH_2$: 75% yield (in 24 h)
R = Ph: 79% yield (in 6 h)

The yield deteriorated to only 20% when the same reaction was performed in refluxing xylene. With more polar solvents such as dioxane, diglyme and *tert*-amyl alcohol, the transformation did not go to completion in 24 h. This is most likely due to inhibition of the ruthenium catalyst by the formed carboxylate which is soluble in more polar solvents, but precipitates as the potassium salt in toluene. Lower conversion of 2-phenylethanol was also observed when the base was changed to LiOH or NaOH, or when the phosphine was replaced by PPh_3 or dppp. A stoichiometric amount of the base is important since the reaction only gave 52% conversion of the alcohol with 0.5 equiv. of KOH. The ruthenium (pre)catalyst **1** could be used in loadings ranging from 0.1 to 2%, but a loading of 1% was often necessary to secure full conversion in 24 h. The conditions were also investigated with benzyl alcohol as the substrate since the oxidation in this case is faster and gave a 79% isolated yield of benzoic acid in only 6 h. However, the yield decreased with a lower catalyst loading or when a higher amount of KOH was used. Attempts to use water as a co-solvent were unsuccessful since the oxidation of a 1 M aqueous solution of benzyl alcohol or 1-butanol in both cases only gave 15% yield of the carboxylic acid. Therefore, the optimized conditions for the oxidation employ 1% of **1**, 1% of $PCy_3 \cdot HBF_4$ and 1.2 equiv. of KOH in refluxing toluene under a flow of argon. The organic solvent allows for an easy isolation of the carboxylic acids which are first precipitated as the potassium salts and then converted into the acids with hydrochloric acid.

With these conditions in hand a number of primary alcohols were subjected to the oxidation to investigate the substrate scope and limitations. First, several *para*-substituted benzyl alcohols were converted into the corresponding benzoic acids (Table 1). The oxidation of *p*-methyl- and *p*-chlorobenzyl alcohol proceeded smoothly and gave the carboxylic acids in high yields (entries 1 and 2). The same transformation with *p*-bromo- and *p*-iodobenzyl alcohol gave slightly lower yields due to a competing dehalogenation to benzoic acid (entries 3 and 4). When *p*-hydroxybenzyl alcohol was submitted to the conditions the oxidation stopped at the aldehyde level and produced *p*-hydroxybenzaldehyde (result not shown). This was also observed with two equiv. of KOH and is presumably due to deprotonation of the phenol. With an ether or a thioether in the *para* position the oxidation again went to the carboxylic acid level (entries 5 and 6). *p*-Phenyl- and *p*-(trifluoromethyl)benzyl alcohol also furnished the corresponding carboxylic acids although in a more moderate yield with the former (entries 7 and 8). In entries 5 – 8 traces of the aldehyde and the corresponding decarbonylation product were also observed by GC-MS. In all the reactions in Table 1 the starting alcohol was fully converted after 6 h. Methyl *p*-(hydroxymethyl)benzoate was also subjected to the oxidation conditions, but in this case only hydrolysis of the ester occurred to produce *p*-(hydroxymethyl)benzoic acid and no oxidation of the alcohol was observed even with an excess of KOH. This is most likely due to precipitation of the potassium salt of *p*-(hydroxymethyl)benzoic acid.

Table 1. Dehydrogenative Oxidation of Benzyl Alcohols to Benzoic Acids[a]

entry	substrate	product	isolated yield (%)
1	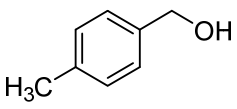	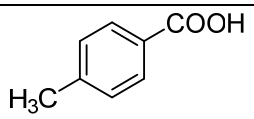	88

2	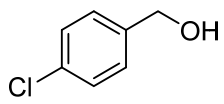	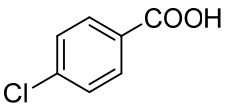	82
3	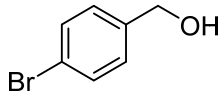	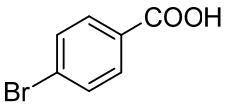	70[b]
4	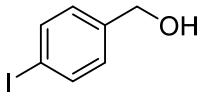	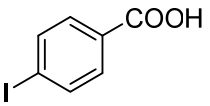	67[c]
5	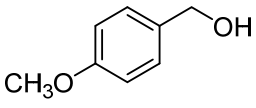	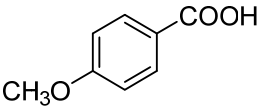	60
6	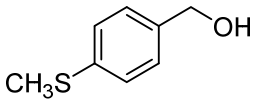	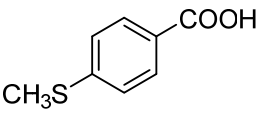	67
7	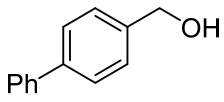	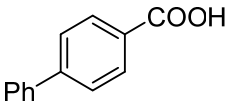	49
8	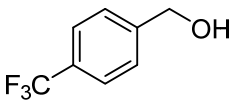	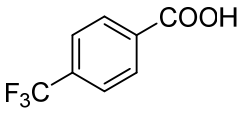	67

[a] Conditions: Alcohol (2.5 mmol), KOH (3 mmol), **1** (0.025 mmol), $PCy_3 \cdot HBF_4$ (0.025 mmol), toluene, reflux, 6 h, then aq. HCl. [b] Benzoic acid also formed in 5% yield. [c] Benzoic acid also formed in 12% yield.

A number of aliphatic primary alcohols were also converted to the corresponding carboxylic acids (Table 2) and in this case a reaction time of 18 h was necessary to secure full conversion since these alcohols are less reactive than the benzylic substrates. Linear alcohols gave good yields (entries 1 and 2) and the same was observed with substituents in the 3 position (entries 3 and 4). Alcohols with substituents in the 2 position gave slightly lower yields (entries 5 – 7) while the dehydrogenation of hex-5-en-1-ol was accompanied by hydrogenation of the olefin (entry 8). Primary alcohols with a chiral center in the 2 position are intriguing substrates since

the stereochemistry may not be retained in the aldehyde intermediate under the basic conditions. Indeed, oxidation of (*S*)-2-methylbutan-1-ol gave fully racemic 2-methylbutanoic acid (entry 9) while (-)-*cis*-myrtanol afforded the thermodynamically more stable (+)-*trans*-dihydromyrtenic acid with complete inversion of stereochemistry (entry 10). No competing aldol condensation from the intermediate aldehyde was observed in any of the examples in Table 2. All the carboxylic acids in Table 1 and 2 were isolated by precipitation of the potassium salts followed by treatment with aqueous hydrochloric acid, extraction with ethyl acetate and removal of the solvent. This yielded sufficiently pure products that did not require further purification by chromatography, distillation or recrystallization.

Table 2. Dehydrogenative Oxidation of Aliphatic Alcohols to Carboxylic Acids[a]

entry	substrate	product	isolated yield (%)
1	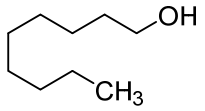	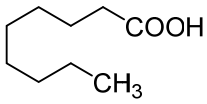	82
2	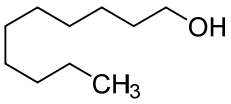	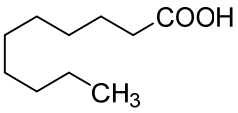	71
3	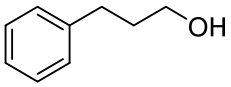	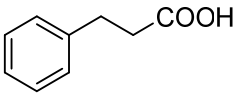	72
4	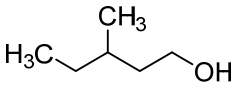	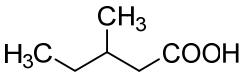	84
5	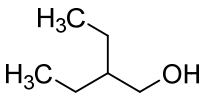	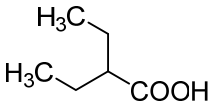	60
6	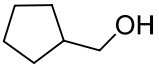	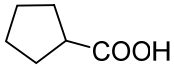	60
7	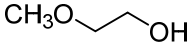	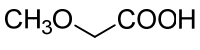	51

8	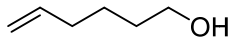	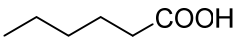	62[b]
9	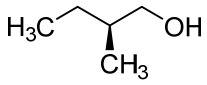	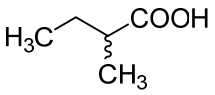	88
10	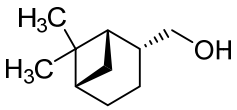	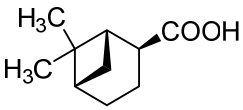	76

[a] Conditions: Alcohol (2.5 mmol), KOH (3 mmol), **1** (0.025 mmol), $PCy_3 \cdot HBF_4$ (0.025 mmol), toluene, reflux, 18 h, then aq. HCl. [b] Yield determined by ^1H NMR.

The evolution of dihydrogen was measured by reacting 1.5 mmol of benzyl alcohol in a Schlenk tube connected to a burette filled with water. A total gas volume of 64 mL was collected, corresponding to approximately 2.7 mmol, which confirms that two equivalents of dihydrogen are released in the reaction (Figure 2).

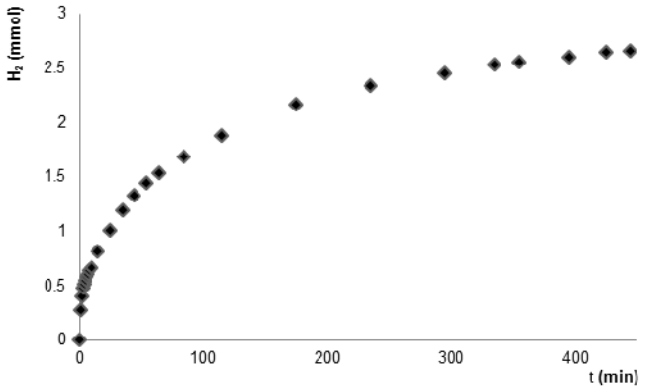

Figure 2. Development of dihydrogen over time.

The intermediate aldehyde was detected when monitoring the oxidation of benzyl alcohol by GC. Actually, in the beginning of the reaction up to 26% of benzaldehyde accumulated in the mixture (Figure 3). The aldehyde is a substrate for the transformation which was shown by subjecting benzaldehyde to the standard oxidation conditions which produced benzoic acid in

72% yield (Scheme 2). Notably, GC measurements of this transformation revealed that benzaldehyde was rapidly converted into a mixture of benzyl alcohol and benzoic acid followed by slow conversion of the alcohol to the acid (Figure 4).

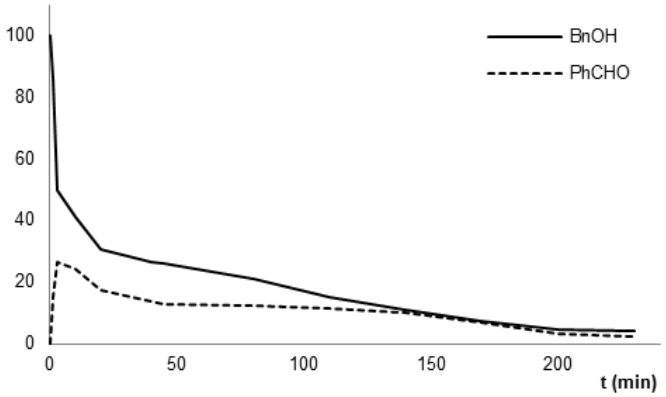

Figure 3. Benzaldehyde formation in the oxidation of benzyl alcohol.

Scheme 2. Dehydrogenative Oxidation of Benzaldehyde

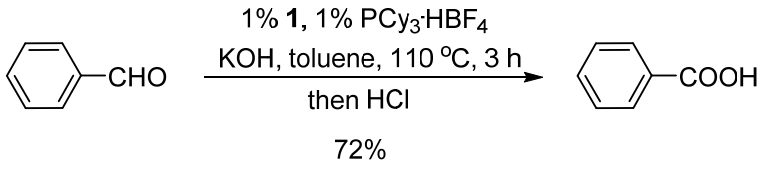

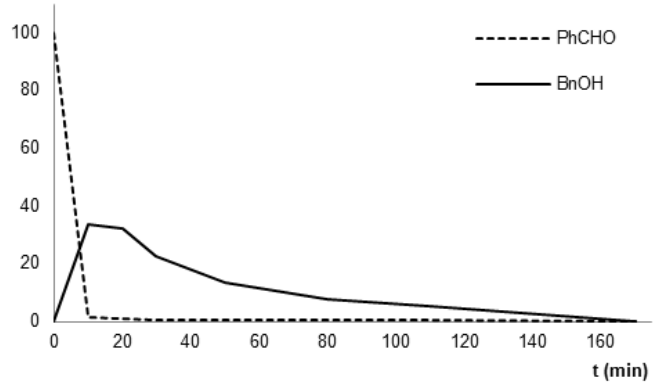

Figure 4. Benzyl alcohol formation in the oxidation of benzaldehyde.

These observations raise the question whether a Cannizzaro reaction is involved in the oxidation of benzyl alcohols.[15] Therefore, benzaldehyde was also reacted with KOH in the absence of complex **1** (Scheme 3). After 1 h the aldehyde was completely consumed and a mixture of benzoic acid and benzyl alcohol was formed according to ^{1}H NMR. This clearly illustrates that the Cannizzaro reaction is possible under the oxidation conditions and it may explain the shorter reaction time with benzyl alcohols as compared to aliphatic alcohols.[16]

Scheme 3. Cannizzaro Reaction with Benzaldehyde

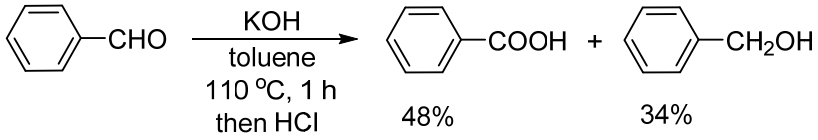

In an attempt to gain more experimental information about the reaction mechanism a Hammett study with *para*-substituted benzyl alcohols was set up in line with our earlier investigations.[14] Unfortunately, it was never possible to obtain a linear correlation between the σ values for the different *para* substituents and the rate constants. This indicates that several mechanistic pathways take part in the overall transformation which again suggests the involvement of the Cannizzaro reaction.

We have previously determined the KIE to 2.29 for the amide synthesis with complex **1** from 1-butanol and benzyl amine.[14] In that case it was necessary to measure the initial rates separately for the deuterated and the non-deuterated alcohols since scrambling of the a protons occurs rapidly when a mixture of labelled and non-labelled alcohol is reacted with complex **1**.[14] The same scrambling was observed when benzyl alcohol-d_2 was allowed to compete with non-

deuterated benzyl alcohol in a reaction with KOH and complex **1** in refluxing toluene. Therefore, the KIE was also in this case measured in a non-competitive manner where 1-butanol was used as the alcohol. In two separate experiments 1-butanol-d_{10} and 1-butanol were reacted with KOD and KOH, respectively, which afforded a KIE of 0.67. This is an unexpectedly low value for a KIE where the deuterated substrates react 1.5 times faster than the non-deuterated counterparts. Since deuteroxide is more basic than hydroxide[17] it may indicate that the basicity or the nucleophilicity of the base is important in the rate-determining step.

To obtain a more detailed knowledge about the reaction pathway a density functional theory (DFT) study was also included in the investigation in line with our earlier work.[14] Since the catalytic system includes a bulky phosphine ligand (PCy_3) it is important to use a functional which takes into account the dispersion interactions. Two well-known functionals B3LYP-D3[18] and M06[19] were investigated where the former in general performed faster while with the latter some optimizations failed to converge. As a consequence, the B3LYP-D3 functional in combination with the LACVP*+ basis set[20] was chosen.

For calculating the Gibbs free energy (ΔG_{tot}), a combination of the gas phase energy of the optimized structure (E_{gas}), single point solution phase energy (E_{sol}) and the Gibbs free energy obtained from the frequency calculations at 383 K (ΔG_{383K}) was used (Eq. 1).[21]

$$\Delta G_{tot} = \Delta G_{383K} + (E_{sol} - E_{gas}) \quad (1)$$

Two phosphine ligands that have similar electronic properties were used in the theoretical studies. For the faster screening of the possible ligand orientations a small PMe_3 ligand was used. To better take into account steric properties of the phosphine ligand, the phosphine used in

the experimental studies (PCy_3) was employed for the calculations of the catalytic cycle. Since it was demonstrated in the experimental studies that the Cannizzaro reaction is a possible pathway for the benzylic alcohols, a simple aliphatic alcohol ethanol was chosen as a model substrate with which the reaction is very likely to proceed exclusively through the ruthenium-catalyzed pathway. Finally, instead of a free hydroxide ion, a hydroxide ion solvated with water molecules was used because it was shown that the addition of water molecules helps to obtain results which are closer to the experimental data.[22] Even though the experiments were conducted with toluene as a solvent, there is still some water present in the system because KOH contains 0.35 – 0.55 equivalents of H_2O per equivalent of the hydroxide depending on the quality of the base (85–90% of KOH in the reactant used in the study). Additionally, the hydroxide ion can be solvated by the alcohol molecules that for simplicity are replaced by the water molecules in the calculations. All these facts allow us to assume that the hydroxide ion involved in the catalytic cycle is always solvated throughout the reaction. It was found that with either two or three water molecules solvating the hydroxide ion, the energy of the step involving the solvated hydroxide remains almost the same. Therefore, a hydroxide ion solvated with two water molecules was used in the computational study.

During the initiation step, the dichloride ruthenium precatalyst **1** loses a molecule of *p*-cymene[14] and based on the literature precedents[23] the two chlorine atoms are believed to be replaced by a hydride and an alkoxide to give a highly electronically unsaturated 12-e^- complex. This complex may be stabilized by coordinating a molecule of the phosphine and a hydroxide ion. The resulting 16-e^- species should have a vacant coordination site *cis* to the alkoxide in order for the β-hydride elimination to proceed. Out of all possible isomers, complex **3** (Scheme 4) with the phosphine ligand in the apical position has the lowest energy. After the β-hydride

elimination, complex **4** should be formed which turns out to be also the most favorable configuration out of all possible isomers of species **4**. These results correlate nicely with our previous studies on the ruthenium-catalyzed dehydrogenative amidation reaction which demonstrated that the apical position for the phosphine ligand is the most favorable in the similar ruthenium complexes.[14] Since complexes **3** and **4** are the most stable species, we decided to continue the studies with the following ligand orientation: the NHC and the phosphine ligands occupy the two apical positions, while an aldehyde (or an alkoxide), a hydroxide ion *cis* to the aldehyde, a hydride *cis* to the hydroxide ion, and another hydride (or an empty spot) *cis* to the hydride all lie in one plane.

Scheme 4. Most Stable Orientation of Ligands in Complexes 3 and 4

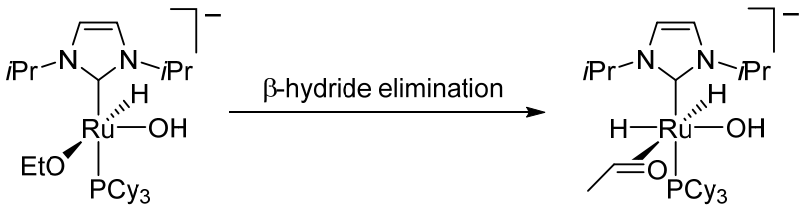

3 **4**

After having determined the orientation of the ligands, the energy profile of the plausible catalytic cycle with PCy_3 instead of PMe_3 was calculated (Scheme 5). After the initiation step the alkoxide-dihydride complex **3** is formed and enters the catalytic cycle. As a formally 16-e^- species **3** is stabilized by the agostic interaction of the ruthenium center with the C–H bond of the α-carbon atom of the alkoxide. This interaction leads to the elongation of the C–H bond by 0.089 Å as compared to the second non-agostic bond at the same carbon atom and consequently facilitates the β-hydride elimination which has the activation barrier of 38.4 $kJ \cdot mol^{-1}$.

Scheme 5. Proposed Catalytic Cycle

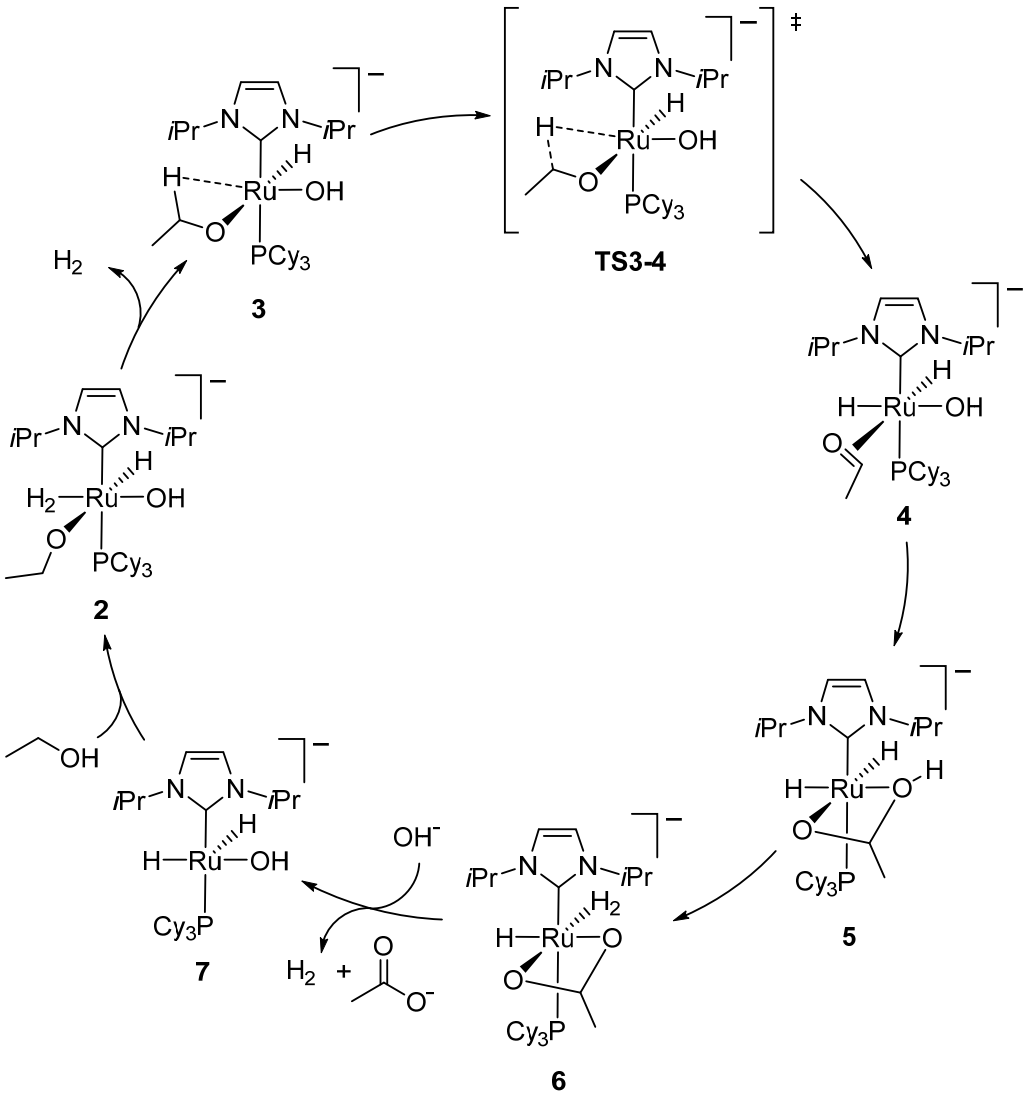

After the β-hydride elimination, complex **4** is formed which contains a molecule of aldehyde bound to ruthenium through the π system of the C=O double bond. Since the hydroxide ligand is coordinated *cis* to the aldehyde, it can act as an internal nucleophile and attack the aldehyde to give a hemiacetal. However, in order for this addition to occur, the aldehyde complex should

isomerize first for the proper alignment of the aldehyde and hydroxide ligands (Scheme 6). This isomerization is exergonic by –11.4 kJ·mol^{-1} and it proceeds through complex **4b** (with the aldehyde bound to ruthenium through the oxygen atom) which is 29.8 kJ·mol^{-1} higher in energy than the starting species **4a**.

Scheme 6. Isomerization of the Aldehyde Complex

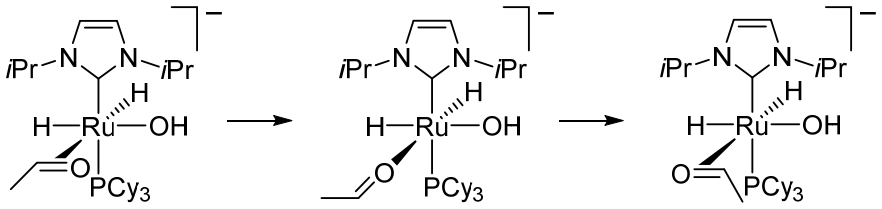

We were unable to locate the transition state for the addition of hydroxide to the aldehyde due to the sharp energy change that accompanied the shift in the coordination mode of the aldehyde during the addition. While in species **4c** the distances between the ruthenium center and the atoms of the carbonyl group is comparable ($r_{Ru–O}$ = 2.280 Å, $r_{Ru–C}$ = 2.213 Å), the Ru–C bond considerably elongates when the hydroxide comes closer to the carbonyl carbon. In order to estimate the energy barrier of the addition, we performed a relaxed coordinate scan with the simultaneous constrains on the distance between the hydroxide oxygen and carbonyl carbon atom as well as the angle between the hydroxide oxygen atom and the C=O double bond (See Supporting Information).

From the coordinate scan, the activation barrier for the addition of the hydroxide can be estimated to be approx. 40 kJ·mol^{-1}. The hemiacetal in species **5** is deprotonated by the *cis*-hydride to give an H_2 complex **6** which exists in equilibrium with a trihydride species (Figure

5). Once this species loses a molecule of H_2, a spontaneous β-hydride elimination occurs to give a carboxylate and complex **7**. All our attempts to locate the transition state for the β-hydride elimination failed, since all geometry optimizations of species **6** without a molecule of H_2 always led to the formation of a carboxylate which implies that the second β-hydride elimination occurs with a high rate and thus cannot be the rate-limiting step.

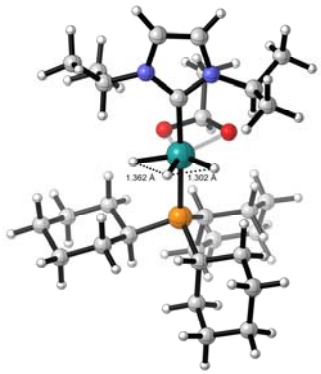

Figure 5. Graphical representation of complex **6**.

After the second β-hydride elimination, the carboxylate dissociates off from the ruthenium center to give a dihydride complex which is stabilized by coordinating one hydroxide ion. Even though the formed complex **7** is coordinatively unsaturated, all five ligands on ruthenium are good electron donors which make species **7** the most stable intermediate of the proposed catalytic cycle (Figure 6). Moreover, the optimization of complex **7** with a molecule of alcohol attached to ruthenium yielded a very long O–Ru distance of 4.180 Å which indicated that the alcohol, being a weak electron donor, does not coordinate to ruthenium. However, after the alcohol has been deprotonated by the hydride, the formed alkoxide is bound to ruthenium to give intermediate **2**.

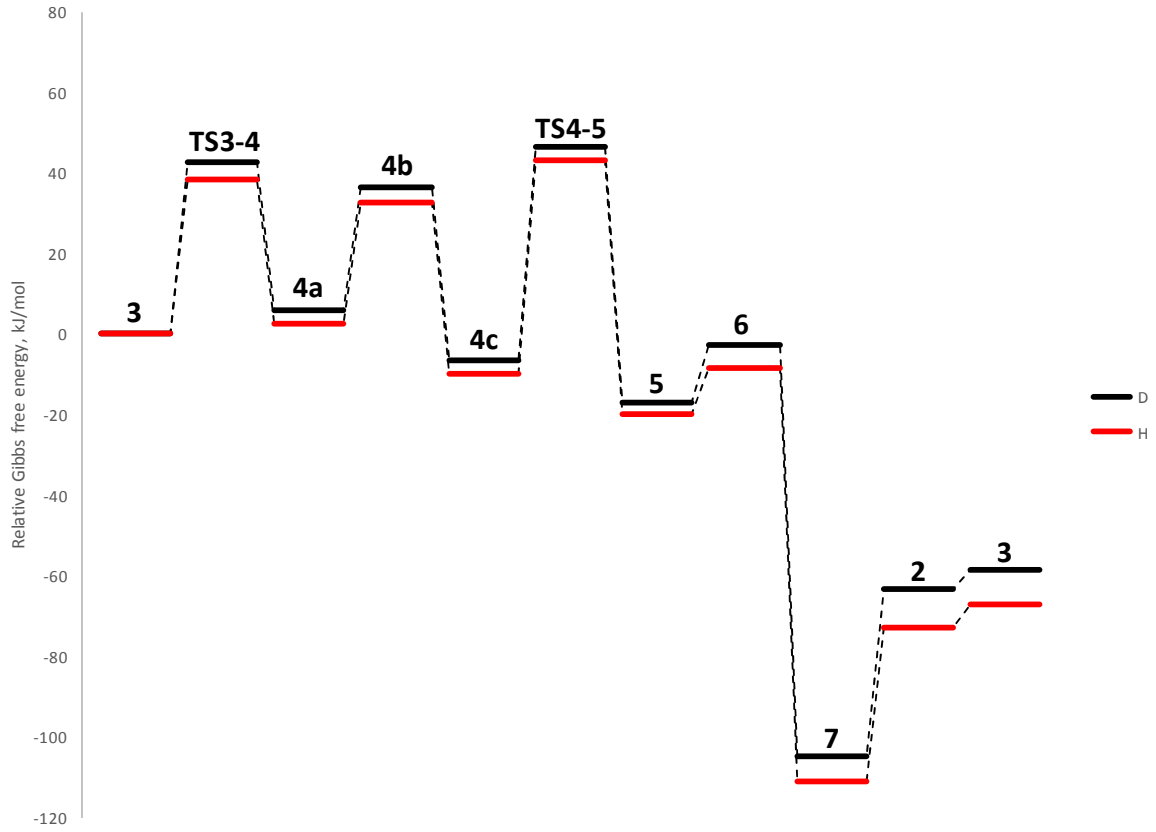

Figure 6. Energy profile for proposed catalytic cycle with fully non-deuterated substrates in red and partially deuterated species at key positions in black.

For the calculation of the kinetic isotope effect the following deuterated species were used: OH^- was replaced with OD^- and CH_3CH_2OH with CH_3CD_2OD. In addition, the hydrogen atoms originating from these two substrates were replaced with deuterium throughout the catalytic cycle. As expected, the first part of the cycle has a higher barrier for the deuterated substrates due to the cleavage of the C–H/D bond (**TS3-4**, 42.8 kJ·mol^{-1} for C–D bond vs. 38.4 kJ·mol^{-1} for C–H bond) which would be expected to result in a significant KIE. Interestingly, later in the catalytic cycle the TS for the addition of the hydroxide (**TS4-5**) has virtually identical barriers (53.0 kJ·mol^{-1} for C–D vs. 52.7 kJ·mol^{-1} for C–H) which could be part of the explanation for

the observed inverse KIE of 0.67. However, since the computed value for this step alone (**TS4-5**) is 1.08 there must be additional contributions to the difference observed with the experimental value such as the difference in basicity and nucleophilicity between hydroxide and deuteroxide.

In summary, we have developed a new protocol for the dehydrogenative synthesis of carboxylic acids which allows for an easy isolation of the products without the use of chromatography, distillation or recrystallization. The reaction is performed in toluene with 1% of complex **1** and a slight excess of KOH. The mechanism was studied computationally and a plausible catalytic cycle identified. The reaction presents an additional application of NHC complex **1** and highlights the value of this species for the development of new dehydrogenative transformations with alcohols.

EXPERIMENTAL SECTION

General Information. All solvents were of HPLC grade and were not further purified. NMR chemical shifts were measured relative to the signals of residual $CHCl_3$ (δ_H 7.26 ppm) and $CDCl_3$ (δ_C 77.16 ppm). HRMS measurements were made using ESI with TOF detection.

General Procedure. A Schlenk tube was charged with complex **1**[11a] (11.5 mg, 0.025 mmol), $PCy_3 \cdot HBF_4$ (9.2 mg, 0.025 mmol), KOH (168 mg, 3 mmol) and a stir bar. A cold finger was attached and the tube was evacuated and refilled three times with argon. The primary alcohol (2.5 mmol) (and sometimes 1.3 mmol of dodecane as internal standard) in toluene (5 mL) was added and the Schlenk tube was placed in a preheated oil bath (T = 120 °C). The reaction was monitored by GC until completion and the Schlenk tube was then removed from the oil bath and cooled to room temperature. Ethyl acetate (5 mL) was added and the white precipitate filtered

off and washed with pentane (15 mL) and ethyl acetate (15 mL). The precipitate was dissolved in water (5 mL) and acidified to pH 1 with saturated aqueous HCl. The aqueous layer was extracted with ethyl acetate (3 × 10 mL). The combined organic layers were dried over Na_2SO_4 and concentrated *in vacuo* to give the corresponding acid as a pure compound by ^{1}H NMR.

Phenylacetic acid (Scheme 1).[24] Isolated as a white solid in 75% yield (255 mg). ^{1}H NMR (400 MHz, DMSO-d_6): δ 3.56 (s, 2H), 7.22–7.33 (m, 5H). ^{13}C NMR (100 MHz, DMSO-d_6): δ 40.7, 126.6, 128.3, 129.4, 135.1, 172.7.

Benzoic acid (Scheme 1).[25] Isolated as a white solid in 79% yield (241 mg). ^{1}H NMR (400 MHz, $CDCl_3$): δ 7.47–7.51 (m, 2H), 7.63 (tt, 2H, J = 1.3, 6.9 Hz), 8.13–8.15 (m, 2H). ^{13}C NMR (100 MHz, $CDCl_3$): δ 128.7, 129.5, 130.4, 134.0, 172.5.

p-*Methylbenzoic acid (Table 1, Entry 1).*[25] Isolated as a light purple solid in 88% yield (300 mg). ^{1}H NMR (400 MHz, DMSO-d_6): δ 2.36 (s, 3H), 7.29 (d, 2H, J = 8.5 Hz), 7.83 (d, 2H, J = 8.5 Hz), 12.77 (brs, 1H). ^{13}C NMR (100 MHz, DMSO-d_6): δ 21.1, 128.0, 129.1, 129.3, 143.0, 167.3.

p-*Chlorobenzoic acid (Table 1, Entry 2).*[25] Isolated as a white solid in 82% yield (321 mg). ^{1}H NMR (400 MHz, DMSO-d_6): δ 7.57 (m, 2H), 7.94 (m, 2H), 13.18 (brs, 1H). ^{13}C NMR (100 MHz, DMSO-d_6): δ 128.8, 129.7, 131.2, 137.8, 166.5.

p-*Bromobenzoic acid (Table 1, Entry 3).*[25] Isolated as a white solid in 70% yield (352 mg). ^{1}H NMR (400 MHz, DMSO-d_6): δ 7.70–7.72 (m, 2H), 7.85–7.87 (m, 2H), 13.18 (brs, 1H). ^{13}C NMR (100 MHz, DMSO-d_6): δ 126.9, 130.0, 131.3, 131.7, 166.6.

p-*Iodobenzoic acid (Table 1, Entry 4).*[25] Isolated as a yellowish solid in 67% yield (415 mg). ^{1}H NMR (400 MHz, DMSO-d_6): δ 7.68–7.70 (m, 2H), 7.88–7.90 (m, 2H), 13.13 (brs, 1H). ^{13}C NMR (100 MHz, DMSO-d_6): δ 101.2, 130.3, 131.1, 137.6, 164.2, 167.0.

p-*Methoxybenzoic acid (Table 1, Entry 5).*[25] Isolated as a white solid in 60% yield (228 mg). ^{1}H NMR (400 MHz, $CDCl_3$): δ 3.88 (s, 3H), 6.93–6.97 (m, 2H), 8.05–8.08 (m, 2H). ^{13}C NMR (100 MHz, $CDCl_3$): δ 55.6, 113.9, 121.8, 132.5, 164.2, 171.2.

p-*(Methylthio)benzoic acid (Table 1, Entry 6).*[3d] Isolated as a yellow pale solid in 67% yield (282 mg). ^{1}H NMR (400 MHz, DMSO-d_6): δ 2.52 (s, 3H), 7.33 (d, 2H, J = 8.5 Hz), 7.85 (d, 2H, J = 8.5 Hz), 12.83 (brs, 1H). ^{13}C NMR (100 MHz, DMSO-d_6): δ 14.0, 124.9, 126.7, 129.7, 144.8, 167.1.

Biphenyl-4-carboxylic acid (Table 1, Entry 7).[26] Isolated as a white solid in 49% yield (243 mg). ^{1}H NMR (400 MHz, DMSO-d_6): δ 7.43 (m, 1H), 7.50 (m, 2H), 7.73 (m, 2H), 7.80 (m, 2H), 8.02 (m, 2H), 12.98 (brs, 1H). ^{13}C NMR (100 MHz, DMSO-d_6): δ 126.8, 126.9, 128.3, 129.1, 129.6, 130.0, 139.0, 144.3, 167.2.

p-*(Trifluoromethyl)benzoic acid (Table 1, Entry 8).*[27] Isolated as a white solid in 67% yield (317 mg). ^{1}H NMR (400 MHz, DMSO-d_6): δ 7.87 (d, 2H, J = 8.2 Hz), 8.13 (d, 2H, J = 8.2 Hz), 13.47 (brs, 1H). ^{13}C NMR (100 MHz, DMSO-d_6): δ 123.8 (q, J = 271.6 Hz), 125.6 (q, J = 3.7 Hz), 130.1, 132.5 (q, J = 32.0 Hz), 134.6, 166.2.

Nonanoic acid (Table 2, Entry 1).[28] Isolated as a colorless oil in 82% yield (324 mg). ^{1}H NMR (400 MHz, $CDCl_3$): δ 0.88 (t, 3H J = 6.7 Hz), 1.27–1.35 (m, 10H), 1.63 (quint, 2H, J = 7.6 Hz), 2.34 (t, 2H, J = 7.6 Hz). ^{13}C NMR (100 MHz, $CDCl_3$): δ 14.2, 22.8, 24.8, 29.2, 29.3, 31.9, 34.2, 180.5.

Decanoic acid (Table 2, Entry 2).[29] Isolated as a colorless oil in 71% yield (306 mg). ^{1}H NMR (400 MHz, $CDCl_3$): δ 0.88 (t, 3H J = 6.9 Hz), 1.21–1.35 (m, 12H), 1.60–1.67 (m, 2H), 2.35 (t, 2H, J = 7.4 Hz). ^{13}C NMR (100 MHz, $CDCl_3$): δ 14.3, 22.8, 24.8, 29.2, 29.4, 29.5, 32.0, 33.9, 178.9.

3-Phenylpropanoic acid (Table 2, Entry 3).[29] Isolated as a white solid in 72% yield (270 mg). ^{1}H NMR (400 MHz, $CDCl_3$): δ 2.65 (m, 2H), 2.92 (t, 2H, J = 7.6 Hz), 7.16–7.28 (m, 5H), 11.55 (brs, 1H). ^{13}C NMR (100 MHz, $CDCl_3$): δ 30.7, 35.8, 126.5, 128.4, 128.7, 140.3, 179.6.

3-Methylpentanoic acid (Table 2, Entry 4).[30] Isolated as a transparent brownish oil in 84% yield (244 mg). ^{1}H NMR (400 MHz, $CDCl_3$): δ 0.90 (t, 3H, J = 7.4 Hz), 0.96 (d, 3H, J = 6.7 Hz), 1.19–1.30 (m, 1H), 1.34–1.45 (m, 1H), 1.83–1.95 (m, 1H), 2.14 (dd, 1H, J = 8.0, 15.0 Hz), 2.35 (dd, 1H, J = 6.0, 15.0 Hz), 11.64 (brs, 1H). ^{13}C NMR (100 MHz, $CDCl_3$): δ 11.4, 19.4, 29.4, 31.9, 41.4, 180.4.

2-Ethylbutyric acid (Table 2, Entry 5).[31] Isolated as a colorless oil in 60% yield (174 mg). ^{1}H NMR (400 MHz, $CDCl_3$): δ 0.94 (t, 6H J = 7.4 Hz), 1.50–1.71 (m, 4H), 2.20–2.27 (m, 1H). ^{13}C NMR (100 MHz, $CDCl_3$): δ 11.9, 24.9, 48.8, 182.8.

Cyclopentanecarboxylic acid (Table 2, Entry 6).[32] Isolated as a colorless oil in 60% yield (171 mg). ^{1}H NMR (400 MHz, $CDCl_3$): δ 1.53–1.96 (m, 8H), 2.72–2.80 (m, 1H), 11.22 (brs, 1H). ^{13}C NMR (100 MHz, $CDCl_3$): δ 25.9, 30.1, 43.8, 183.5.

Methoxyacetic acid (Table 2, Entry 7).[33] Isolated as a colorless oil in 51% yield (115 mg). ^{1}H NMR (400 MHz, $CDCl_3$): δ 3.45 (s, 3H), 4.07 (s, 2H), 9.66 (brs, 1H). ^{13}C NMR (100 MHz, $CDCl_3$): δ 59.5, 69.3, 175.4.

Hexanoic acid (Table 2, Entry 8).[29] Isolated as a colorless oil in 66% yield (192 mg) (includes 4% of 5-hexenoic acid according to NMR). ^{1}H NMR (400 MHz, $CDCl_3$): δ 0.88–0.92 (m, 3H), 1.28–1.36 (m, 4H), 1.60–1.68 (m, 2H), 2.35 (t, 2H, J = 7.6 Hz). ^{13}C NMR (100 MHz, $CDCl_3$): δ 14.0, 22.4, 24.5, 31.3, 34.2, 180.4.

2-Methylbutanoic acid (Table 2, Entry 9).[34] Isolated as a colorless oil in 88% yield (225 mg). ^{1}H NMR (400 MHz, $CDCl_3$): δ 0.95 (t, 3H, J = 7.0 Hz), 1.18 (d, 3H, J = 7.5 Hz), 1.45–1.55 (m,

1H), 1.66–1.77 (m, 1H), 2.36–2.44 (m, 1H). ^{13}C NMR (100 MHz, $CDCl_3$): δ 11.7, 16.5, 26.7, 41.0, 183.6.

*(1*S*,2*S*,5*S*)-6,6-Dimethylbicyclo[3.1.1]heptane-2-carboxylic acid (Table 2, Entry 10).* Isolated as a brownish sheer oil in 76% yield (321 mg). $[\alpha]_D$ +1.9 (*c* 1.0, EtOAc). ^{1}H NMR (400 MHz, $CDCl_3$): δ 0.87 (s, 3H), 1.23 (s, 3H), 1.53 (d, 1H, J = 10.0 Hz), 1.70–1.80 (m, 1H), 1.83–1.92 (m, 3H), 2.03–2.21 (m, 3H), 2.93 (t, 1H, J = 9.0 Hz). ^{13}C NMR (100 MHz, $CDCl_3$): δ 16.7, 20.4, 23.9, 24.3, 26.5, 39.3, 40.2, 41.3, 43.8, 183.3. HRMS: *m*/*z* calcd for $C_{10}H_{17}O_2$ 169.1223 $[M + H]^+$, found 169.1217.

Computational Details. All calculations were performed in Jaguar[35] by using the Maestro graphical interface.[36] All of the structures were optimized in the gas phase and the single-point solvation energy was calculated for the optimized structures by using a standard Poisson–Boltzmann solver with suitable parameters for toluene as the solvent (dielectric constant: ε = 2.379, probe radius: r = 2.707 Å). Gibbs free energies were obtained from the vibrational-frequency calculations for the gas-phase geometries at 298 K and 383 K. All of the transition states were characterized by the presence of one negative vibrational frequency. Graphical representation of the calculated structures was made in CYLview.[37]

ACKNOWLEDGMENT

We thank the Danish Council for Independent Research – Technology and Production Sciences for financial support (grant 09-066621).

Supporting Information. Determination of the KIE, copies of ^{1}H and ^{13}C NMR spectra as well as Cartesian coordinates and energies for the calculated structures. This material is available free of charge via the Internet at http://pubs.acs.org.

References

1) Tojo, G.; Fernández, M. *Oxidation of Primary Alcohols to Carboxylic Acids – A Guide to Current Common Practice*, Springer, **2007**.
2) Gunanathan, C.; Milstein, D. *Science* **2013**, *341*, 1229712.
3) (a) Gianetti, T. L.; Annen, S. P.; Santiso-Quinones, G.; Reiher, M.; Driess, M.; Grützmacher, H. *Angew. Chem. Int. Ed.* **2016**, *55*, 1854–1858. (b) Trincado, M.; Grützmacher, H.; Vizza, F.; Bianchini, C. *Chem. Eur. J.* **2010**, *16*, 2751–2757. (c) Annen, S.; Zweifel, T.; Ricatto, F.; Grützmacher, H. *ChemCatChem* **2010**, *2*, 1286–1295. (d) Zweifel, T.; Naubron, J.-V.; Grützmacher, H. *Angew. Chem. Int. Ed.* **2009**, *48*, 559–563.
4) Balaraman, E.; Khaskin, E.; Leitus, G.; Milstein, D. *Nat. Chem.* **2013**, *5*, 122–125.
5) Hu, P.; Ben-David, Y.; Milstein, D. *J. Am. Chem. Soc.* **2016**, *138*, 6143–6146.
6) Li, H.; Hall, M. B. *J. Am. Chem. Soc.* **2014**, *136*, 383–395.
7) Malineni, J.; Keul, H.; Möller, M. *Dalton Trans.* **2015**, *44*, 17409–17414.
8) (a) Zhang, L.; Nguyen, D. H.; Raffa, G.; Trivelli, X.; Capet, F.; Desset, S.; Paul, S.; Dumeignil, F.; Grauvin, R. M. *ChemSusChem* **2016**, *9*, 1413–1423. (b) Choi, J.-H.; Heim, L. E.; Ahrens, M.; Prechtl, M. H. G. *Dalton Trans.* **2014**, *43*, 17248–17254.
9) Sponholz, P.; Mellmann, D.; Cordes, C.; Alsabeh, P. G.; Li, B.; Li, Y.; Nielsen, M.; Junge, H.; Dixneuf, P.; Beller, M. *ChemSusChem* **2014**, *7*, 2419–2422.

10) Sawama, Y.; Morita, K.; Asai, S.; Kozawa, M.; Tadokoro, S.; Nakajima, J.; Monguchi, Y.; Sajiki, H. *Adv. Synth. Catal.* **2015**, *357*, 1205–1210.

11) (a) Dam, J. H.; Osztrovszky, G.; Nordstrøm, L. U.; Madsen, R. *Chem. Eur. J.* **2010**, *16*, 6820–6827. (b) Nordstrøm, L. U.; Vogt, H.; Madsen, R. *J. Am. Chem. Soc.* **2008**, *130*, 17672–17673.

12) (a) Makarov, I S.; Madsen, R. *J. Org. Chem.* **2013**, *78*, 6593–6598. (b) Sølvhøj, A.; Madsen, R. *Organometallics* **2011**, *30*, 6044–6048.

13) Maggi, A.; Madsen, R. *Organometallics* **2012**, *31*, 451–455.

14) Makarov, I. S.; Fristrup, P.; Madsen, R. *Chem. Eur. J.* **2012**, *18*, 15683–15692.

15) An intramolecular Cannizzaro reaction (through a 1,2-hydride shift) has previously been proposed in the conversion of glycerol and trioses to lactate, see: (a) Sharninghausen, L. S.; Campos, J.; Manas, M. G.; Crabtree, R. H. *Nat. Commun.* **2014**, *5*, 5084. (b) Pescarmona, P. P.; Janssen, K. P. F.; Delaet, C.; Stroobants, C.; Houthoofd, K.; Philippaerts, A.; De Jonghe, C.; Paul, J. S.; Jacobs, P. A.; Sels, B. F. *Green Chem.* **2010**, *12*, 1083–1089.

16) In our previous syntheses of amides and esters with complex **1** benzyl alcohols were converted more slowly than linear aliphatic alcohols, see ref. 11 and 12.

17) Walters, E. A.; Long, F. A. *J. Phys. Chem.* **1972**, *76*, 362–365.

18) (a) Grimme, S.; Antony, J.; Ehrlich, S.; Krieg, H. *J. Chem. Phys.* **2010**, *132*, 154104. (b) Becke, A. D. *J. Chem. Phys.* **1993**, *98*, 5648–5652. (c) Lee, C.; Yang, W.; Parr, R. G. *Phys. Rev. B* **1988**, *37*, 785–789.

19) Zhao, Y.; Truhlar, D. G. *Theor. Chem. Acc.* **2008**, *120*, 215–241.

20) Hay, P. J.; Wadt, W. R. *J. Chem. Phys.* **1985**, *82*, 270–283.

21) (a) Fristrup, P.; Tursky, M.; Madsen, R. *Org. Biomol. Chem.* **2012**, *10*, 2569–2577. (b) Lau, J. K.-C.; Deubel, D. V. *J. Chem. Theory Comput.* **2006**, *2*, 103–106. (c) Wertz, D. H. *J. Am. Chem. Soc.* **1980**, *102*, 5316–5322.

22) Bryantsev, V. S.; Diallo, M. S.; van Duin, A. C. T.; Goddard, W. A., III *J. Chem. Theory Comput.* **2009**, *5*, 1016–1026.

23) Solari, E.; Gauthier, S.; Scopelliti, R.; Severin, K. *Organometallics* **2009**, *28*, 4519–4526.

24) Zhou, G.-B.; Zhang, P.-F.; Pan, Y.-J. *Tetrahedron* **2005**, *61*, 5671–5677.

25) Kobayashi, K.; Kondo, Y. *Org Lett.* **2009**, *11*, 2035–2037.

26) Du, Z.; Zhou, W.; Wang, F.; Wang, J.-X. *Tetrahedron* **2011**, *67*, 4914–4918.

27) Berger, P.; Bessmernykh, A.; Caille, J.-C.; Mignonac, S. *Synthesis* **2006**, 3106–3110.

28) Zimmermann, F.; Meux, E.; Mieloszynski, J.-L.; Lecuire, J.-M.; Oget, N. *Tetrahedron Lett.* **2005**, *46*, 3201–3203.

29) Saisaha, P.; Buettner, L.; van der Meer, M.; Hage, R.; Feringa, B. L.; Browne, W. R.; de Boer, J. W. *Adv. Synth. Catal.* **2013**, *355*, 2591–2603.

30) Yabuuchi, T.; Kusumi, T. *J. Org. Chem.* **2000**, *65*, 397–404.

31) Lafrance, D.; Bowles, P.; Leeman, K.; Rafka, R. *Org. Lett.* **2011**, *13*, 2322–2325.

32) Zhao, J.; Mück-Lichtenfeld, C.; Studer, A. *Adv. Synth. Catal.* **2013**, *355*, 1098–1106.

33) (a) Barelle, M.; Béguin, C.; Tessier, S. *Org. Magn. Reson.* **1982**, *19*, 102–104. (b) Ray, W. J.; Katon, J. E.; Krause, P. F. *Appl. Spectrosc.* **1979**, *33*, 492–495.

34) Kawashima, M.; Sato, T.; Fujisawa, T. *Tetrahedron* **1989**, *45*, 403–412.

35) Jaguar, version 9.0, Schrodinger, Inc., New York, NY, **2015**.

36) Bochevarov, A. D.; Harder, E.; Hughes, T. F.; Greenwood, J. R.; Braden, D. A.; Philipp, D. M.; Rinaldo, D.; Halls, M. D.; Zhang, J.; R. Friesner, A. *Int. J. Quantum Chem.* **2013**, *113*, 2110–2142.

37) CYLview, version 1.0b, Legault, C.Y.; Université de Sherbrooke, **2009**.